Identification of unavoided crossings in nonadiabatic photoexcited dynamics involving multiple electronic states in polyatomic conjugated molecules

Sebastian Fernandez-Alberti,[1,a] Adrian E. Roitberg,[2] Tammie Nelson,[3] and Sergei Tretiak[3]
[1]*Universidad Nacional de Quilmes, Roque Saenz Peña 352, B1876BXD Bernal, Argentina*
[2]*Quantum Theory Project, Department of Chemistry, University of Florida, Gainesville, Florida 32611, USA*
[3]*Theoretical Division, Center for Nonlinear Studies (CNLS), and Center for Integrated Nanotechnologies (CINT), Los Alamos National Laboratory, Los Alamos, New Mexico 87545, USA*

(Received 27 February 2012; accepted 18 June 2012; published online 6 July 2012)

Radiationless transitions between electronic excited states in polyatomic molecules take place through unavoided crossings of the potential energy surfaces with substantial non-adiabatic coupling between the respective adiabatic states. While the extent in time of these couplings are large enough, these transitions can be reasonably well simulated through quantum transitions using trajectory surface hopping-like methods. In addition, complex molecular systems may have multiple "trivial" unavoided crossings between noninteracting states. In these cases, the non-adiabatic couplings are described as sharp peaks strongly localized in time. Therefore, their modeling is commonly subjected to the identification of regions close to the particular instantaneous nuclear configurations for which the energy surfaces actually cross each other. Here, we present a novel procedure to identify and treat these regions of unavoided crossings between non-interacting states using the so-called Min-Cost algorithm. The method differentiates between unavoided crossings between interacting states (simulated by quantum hops), and trivial unavoided crossings between non-interacting states (detected by tracking the states in time with Min-Cost procedure). We discuss its implementation within our recently developed non-adiabatic excited state molecular dynamics framework. Fragments of two- and four-ring linear polyphenylene ethynylene chromophore units at various separations have been used as a representative molecular system to test the algorithm. Our results enable us to distinguish and analyze the main features of these different types of radiationless transitions the molecular system undertakes during internal conversion. © *2012 American Institute of Physics*. [http://dx.doi.org/10.1063/1.4732536]

I. INTRODUCTION

The computational simulation of photodynamical processes involving radiationless transitions between multiple excited states in polyatomic molecules is one of the main goals in the field of molecular organic photochemistry.[1–5] In the last decade, direct nonadiabatic molecular dynamics (NA-MD) simulations[6–8] have been playing an important role in the study of photochemical and photophysical deactivation mechanisms in organic compounds.[9–13] Furthermore, *ab initio* NA-MD have been successfully applied to study ultrafast photoinduced electron transfer (ET) processes[14,15] in quantum dots,[16,17] and Auger phenomena including multiple exciton generation and recombination.[18] Among these methods, trajectory surface hopping algorithms have proven to be efficient techniques to describe the photochemistry of a variety of organic molecules such as benzene,[19] fulvene, azulene,[20] nucleobases,[21–23] poly(phenylene ethynylene) dendrimers,[74,75] formamide,[24] silaethylene,[25] ethylene,[26] azobenzene,[27,28] azomethane,[29] cyclopropanone,[30] and pyrrole[31,32] among others. Complexity of the excited state electronic energies, gradients, and nonadiabatic couplings greatly varies for different molecular systems. Several of these studies have shown that avoided and unavoided crossings between excited electronic state potential energy surfaces (PESs) have significant effects on the efficiencies of internal vibrational and electronic relaxation processes after the initial photoexcitation.[33,34]

In polyatomic molecules the "non-crossing rule" looses its validity and every two-state crossing is an unavoided crossing, which leads to the formation of a conical intersection near state degeneracy. A classification of the most common types of conical intersection has been previously reported by Worth and Cederbaum.[34] If the cone formed by adiabatic PESs is steep, the excited wavepacket trajectory might go through/near the tip of the cone as it is the case of rhodopsin isomerization.[35–38] In contrast, if the cone is flat (or, more generally, the intersecting PESs have similar gradients), the wavepacket trajectory will likely miss the conical intersection seam. In both cases, the transition between states occurs due to non-adiabatic coupling of the respective adiabatic state wavefunctions. This scenario, typical for internal conversion in polyatomic molecules with multiple excited states, has been previously classified as weakly or strongly avoided crossings along the effective reaction coordinate.[4,5,34]

[a]Author to whom correspondence should be addressed. Electronic mail: sfalberti@gmail.com.

Special cases of unavoided crossings can also take place between two noninteracting states of the polyatomic molecule. In such cases, denoted as "trivial" unavoided crossings, the nonadiabatic couplings are described as sharp peaks strongly localized on the proximity of the exact crossing points. Therefore, while becoming near infinity at the exact crossing point, they vanish elsewhere. In the present article we show that this may be realized in the case when parts of the molecular system are spatially separated and their wavefunctions have vanishing interactions.[64,74] Here the wavepacket trajectory must cross the conical intersection seam following the "diabatic pathway" of its parent wavefunction along the respective adiabatic PES. Nowadays it is well accepted that the excited-state molecular dynamics of any polyatomic molecular compound is likely to experience multiple regions of PESs crossings within its excited-state lifetime. Consequently, either weakly or strongly avoided crossings, as well as unavoided crossings between interacting or noninteracting states are common events during radiationless vibronic relaxation. We show that NA-MD simulations that do not treat the trivial unavoided crossings properly may give rise to serious artefacts in the results.

While the extent in time of couplings between interacting adiabatic states are large enough, either weakly or strong avoided crossings as well as unavoided crossings along the effective vibrational coordinates have been shown to be well simulated using various trajectory surface hopping algorithms.[77] In contrast, the treatment of "trivial" unavoided crossings introduces the additional difficulty that implies their identification. In the simplest case of crossings of excited state PESs of two non-interacting molecules separated by a large distance, the miss of a "trivial" unavoided crossing may lead to unphysical long range energy transfer processes in numerical simulations. Because of such crossings, the assignment of the adiabatic states based on the energy-ordering criterion at each time during dynamics becomes useless and the identities of the adiabatic state wavefunctions must be followed. Most of these methods require identification of regions close to the particular instantaneous nuclear configurations for which the PESs actually cross each other. Different strategies have been proposed to deal with such regions of unavoided crossings within direct nonadiabatic molecular dynamics simulations using trajectory surface hopping algorithms. Thresholds for the energy gap between states and the non-adiabatic coupling terms (NACTs) have been used to propose approximate alternatives to the Tully's fewest-switches algorithm,[77] although the uncertainty in the calculation of NACTs at nuclear configurations close to the crossing points can introduce large inaccuracies in the use of the NACTs magnitudes to detect crossing regions. Unavoided crossings can also be detected through the unphysical discontinuities in the potential energy surfaces and gradients observed in the case of state degeneracies.[39] Nevertheless, this scheme is restricted to microcanonical ensembles (NVE) and cannot be applied for Langevin dynamics or molecular dynamics at constant temperature.

A threshold related to the energy gap between crossing states has also been used as a switch to trigger an explicit track of states at two different integration time steps in order to maximize their overlap.[64] While the difference in energy is not an unequivocal criterion to alert about a potential interaction between states, the method has been successfully applied to a variety of small and middle-size organic molecules. However, the application of such procedure to the simulation of the photodynamics of large organic molecules dealing with multiple excited states (twenty or more) requires an efficient procedure or algorithm able to track the states explicitly. Recent improvements in this direction has been achieved by using an original assignment algorithm to minimize the difference between two local diabatic expansions while applying the interpolating approaches of the potential energy surfaces during direct NA-MD simulations.[40] Alternatively, the same can be accomplished through a transformation of the adiabatic states to a "locally diabatic" representation, i.e., to a set of electronic states which are specifically diabatic along a particular nuclear trajectory.[13] The corresponding unitary transformation and the Hamiltonian in the diabatic basis are obtained from the overlap between the adiabatic wavefunctions of adjacent time steps. Therefore, both quantities depend on the accuracy of numerical calculations of NACTs. In the last few years, an analytical calculation of NACTs[41,42,60] (as opposed to the much slower numerical differentiation) has introduced a significant improvement in the accuracy and computational efficiency of these quantities. Thus, there is a clear need for an algorithm that relies on the analytical NACTs while identifying crossings events in order to allow the electronic populations to follow the corresponding diabatic pathway.

In this article, we present a novel procedure to identify crossing events using the so-called Min-Cost assignment algorithm, originally used for complex optimization problems in economics. Such Min-Cost algorithm has been successfully applied to track the identity of instantaneous normal modes during the simulation of intramolecular vibrational dynamics of polyatomic molecules in solution.[66,77] The method is suitable to be used for direct NA-MD simulations using trajectory surface hopping algorithms that involve a large number of coupled electronically excited states. It allows a differentiation between unavoided crossings involving interacting states (simulated by quantum hops) and "trivial" unavoided crossings between non-interacting states (detected by explicit tracking of the states in time). We discuss in detail its implementation within our recently developed Non-Adiabatic Excited-State Molecular Dynamics (NA-ESMD)[60] framework suitable for dealing with photoinduced dynamics in large molecular systems on the time scales of tens of picoseconds. The NA-ESMD method characterizes the excited state PESs by calculating *on the fly* excited-state energies, gradients and respective non-adiabatic coupling terms. It combines classical molecular dynamics with quantum transitions (MDQT)[47,48] using the fewest switches criterion[48] and Langevin dynamics[43] algorithms. The method has been successfully applied to simulate the ultrafast vibrational and electronic energy transfer between linear poly(phenylene ethynylene) (PPE) units[44,74,75] and molecular internal energy conversion followed photoexcitation. In order to test the efficiency of our treatment of trivial unavoided crossings, in this paper we apply the NA-ESMD method to treat cases in which the PPE units are separated at different distances.

The paper is organized as follows. In Sec. II, a brief background of the NA-ESMD framework and transition densities calculations is provided as well as a detailed description of the procedure to identify unavoided crossing events and transfer the electronic population following the corresponding diabatic pathway. In Sec. III, we present and discuss our findings related to the testing of the method for different intermolecular distances between our model PPE molecules. Conclusions are given in Sec. IV.

II. METHODS

A. The NA-ESMD background

The non-adiabatic excited-states molecular dynamics (NA-ESMD) approach[45,46,60] can be used to simulate photoinduced dynamics[6] in large organic conjugated molecules involving multiple coupled electronic excited states.[74,75] Here molecular dynamics with quantum transitions (MDQT) (Refs. 47 and 49) approach is combined with "*on the fly*" analytical calculations of excited state energies,[50–52] gradients[53,54,60] and non-adiabatic coupling[42,55,60] terms. The Collective Electron Oscillator (CEO) method[50,55,56] applied at the Austin Model 1 (AM1) (Ref. 59) semiempirical level in combination with the Configuration Interaction Singles (CIS) formalism is used to describe correlated excited states. More details related to NA-ESMD implementations, advantages, and testing parameters can be found elsewhere.[60,61]

Our MDQT implementation considers the simultaneous propagation of an electronic wavepacket quantum mechanically while the nuclei move classically on a potential energy surface defined by a single AM1/CIS electronic state at a given time. Transitions from one electronic surface to another are allowed depending on the strength of their non-adiabatic couplings. The electronic wavefunction $\boldsymbol{\psi}(\boldsymbol{r}, \boldsymbol{R}, t)$ represents a superposition state expanded in terms of the CIS adiabatic functions $\boldsymbol{\phi}_\alpha(\boldsymbol{r}; \boldsymbol{R}(t))$ as

$$\boldsymbol{\psi}(\boldsymbol{r}, \boldsymbol{R}, t) = \sum_\alpha c_\alpha(t)\boldsymbol{\phi}_\alpha(\boldsymbol{r}; \boldsymbol{R}(t)). \tag{1}$$

With α being the excited state label, $c_\alpha(t)$ are the time-dependent CIS expansion coefficients, and $\boldsymbol{r}$ and $\boldsymbol{R}$ are the electronic and nuclear coordinates, respectively. Therefore, the coupled equations of motion for the $c_\alpha(t)$ coefficients are obtained by substituting eq. (1) into the time-dependent Schrödinger equation yielding the following expression:

$$i\hbar\frac{\partial c_\alpha(t)}{\partial t} = c_\alpha(t)E_\alpha - i\hbar\sum_{\beta\neq\alpha} c_\beta(t)\,\dot{\mathbf{R}}\cdot\mathbf{d}_{\alpha\beta}, \tag{2}$$

where E_α is the α^{th} eigenvalue of the CIS matrix calculated at time t, and $\mathbf{d}_{\alpha\beta}$ is the non-adiabatic coupling vector defined by $\mathbf{d}_{\alpha\beta} = \langle\boldsymbol{\phi}_\alpha(\boldsymbol{r}; \boldsymbol{R}(t)) \mid \nabla_R\boldsymbol{\phi}_\beta(\boldsymbol{r}; \boldsymbol{R}(t))\rangle$, and

$$\dot{\mathbf{R}}\cdot\mathbf{d}_{\alpha\beta} = \left\langle\boldsymbol{\phi}_\alpha(\boldsymbol{r}; \boldsymbol{R}(t)) \,\middle|\, \frac{\partial\boldsymbol{\phi}_\beta(\boldsymbol{r}; \boldsymbol{R}(t))}{\partial t}\right\rangle \tag{3}$$

is the time-dependent non-adiabatic coupling (NACT) with $\dot{\mathbf{R}} = \nabla_t\mathbf{R}$ being the nuclear velocities.

B. Analysis of the spatial localization of electronic transition densities

Vertical transition energies $\Omega_\alpha = E_\alpha - E_g$ (where E_g (E_α) is the ground- (excited-) state energy) and the corresponding transition density matrices $(\rho^{g\alpha})_{nm} \equiv \langle\boldsymbol{\phi}_\alpha(\boldsymbol{r}; \boldsymbol{R}(t))|c_m^+c_n|\boldsymbol{\phi}_g(\boldsymbol{r}; \boldsymbol{R}(t))\rangle$ (denoted *electronic normal modes*) are computed according to the CEO procedure.[62,63] c_m^+ (c_n) are creation (annihilation) operators; and n and m refer to atomic orbital (AO) basis functions. The diagonal element of $(\rho^{g\alpha})_{nn}$ represents the net change in the distribution of the electronic density induced on the nth atomic orbital when the molecule undergoes the g to α electronic transition, and therefore, $(\rho^{g\alpha})_{nn}$ values are directly relevant to the optically induced changes. Furthermore, at the CIS approximation, matrices $(\rho^{g\alpha})_{nm}$ are the eigenvectors of the tetradic CIS matrix in the orthogonal atomic orbital representation with the usual normalization condition $\sum_{n,m}(\rho^{g\alpha})^2_{nm} = 1$.[52,60] In order to obtain the fraction of the transition density localized on each linear PPE unit (i.e., two-ring, three-ring, and four-ring para-substituted phenylene ethynylene units, see Figure 1), we sum up the atomic contributions belonging to each of them as

$$(\rho^{g\alpha})^2_{X\text{-ring}} = \sum_{n_A m_A}(\rho^{g\alpha})^2_{n_A m_A} + \left(\sum_{n_A m_B}(\rho^{g\alpha})^2_{n_A m_B} + \sum_{n_B m_A}(\rho^{g\alpha})^2_{n_B m_A}\right) + \frac{1}{2}\sum_{n_B m_B}(\rho^{g\alpha})^2_{n_B m_B}, \tag{4}$$

where the index A runs over all atoms localized in the X-ring (X = 2, 3, 4) linear PPE unit, and the index B runs over atoms localized in between these units. Consequently, in our case $\sum_X(\rho^{g\alpha})^2_{X\text{-ring}} \approx 1$ since meta-conjugation blocks long-range electronic interactions.

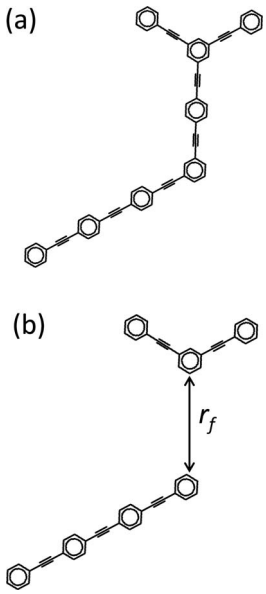

FIG. 1. (a) Chemical structure of the dendritic molecule consisting of two two-ring, one three-ring, and one four-ring linear poly(phenylene ehynylene) (PPE) units linked by meta-substitution. (b) Fragments of the dendrite (2,2-PPE and 4-PPE molecules) used to test the numerical procedure to identify unavoided crossings.

C. Identification of unavoided crossings

During photoexcited dynamics, multiple unavoided crossings between many coupled excited electronic states make it impossible to use energy ordering to identify the states. Trivial unavoided crossings between non-interacting states lead to changes in the energy order of the states. At the critical geometries corresponding to instantaneous nuclear configurations for which two energy surfaces come close together in energy and actually cross each other, both states become quasi-degenerate and the nonadiabatic coupling between them becomes very large (according to the Helmann-Feynman theorem, $|\mathbf{d}_{\alpha\beta}|$ is proportional to $1/\Delta E_{\alpha\beta}$).[42] Therefore, practically the entire electronic populations are interchanging between the corresponding adiabatic states. During the NA-ESMD simulations, the nuclear motion throughout an unavoided crossing should lead to a unit probability that the system remains on the same diabatic state. Within the MDQT approach, transition from one electronic surface to another guarantees that the classical population is well behaved. However, either the numerical propagations of quantum and classical degrees of freedom using the finite values of time steps or the sharp peaks strongly localized in time experienced by the nonadiabatic couplings could lead to transitions missed by the model. This failure can lead to unphysical sudden changes in the spatial localization of the transition density of the current state.

In order to avoid this problem it is necessary to track the identities of the states over time.[64] New states at the current time step i are assigned in terms of old states at the preceding time step (i-1). The correspondence between both sets of states can be based on the highest values of their overlaps. The maximum overlaps are obtained through the maximization of the trace of the square of the overlap matrix $\mathbf{S}$ whose elements are defined as the dot product

$$\begin{aligned} s_{\beta\alpha}(t; t+\Delta t) &\equiv \boldsymbol{\phi}_\beta(\boldsymbol{r}; \boldsymbol{R}(t)) \cdot \boldsymbol{\phi}_\alpha(\boldsymbol{r}; \boldsymbol{R}(t+\Delta t)) \\ &= \sum_{n,m} \rho^{g\beta}(t)_{nm} \rho^{g\alpha}(t+\Delta t)_{mn}, \end{aligned} \tag{5}$$

where Δt is the classical time step used during the NA-ESMD simulations. This can be done by selecting those elements of the $\mathbf{S}(t; t+\Delta t)$ matrix, one for each row, and each pertaining to a different column (or vice versa), which maximize the sum of their squared values. This is a well-known problem in Economics known as the min-cost or min-sum assignment problem, which, in general, states the following: given an N x N cost matrix $\mathbf{C} = \{c_{ij}\}$ with $c_{ij} \geq 0$ for all i and j, assign each row to one column, and vice versa, so as to minimize the cost given by the sum of the row-column assignments. The Min-Cost assignment problem consists therefore of finding a permutation (f_α) of the integers 1, 2, ..., N which minimizes the trace z given by

$$z = \sum_{\alpha=1}^{N} c_{\alpha, f_\alpha}, \tag{6}$$

and can be efficiently solved using the so-called Hungarian method.[65] Following previous applications of the method to assign vibrational states,[66,67] we adopt the code given by Toth *et al.*[65] For a given matrix, this code in fact provides a set of elements, each one belonging to a different row and column, whose sum is minimal. So, in order to maximize z, as required in our case, we apply the code to the matrix formed by the negative values of the $s^2_{\beta\alpha}(t; t+\Delta t)$ elements, that is, we set $c_{ij} = -s^2_{\beta\alpha}(t; t+\Delta t)$.

As it has been previously discussed,[67] the direct Min-Cost assignment method of the $\boldsymbol{\phi}_\alpha(\boldsymbol{r}; \boldsymbol{R}(t+\Delta t))$ adiabatic state may potentially lead to unphysical assignment of $\boldsymbol{\phi}_\alpha(\boldsymbol{r}; \boldsymbol{R}(t+\Delta t))$ state to $\boldsymbol{\phi}_\beta(\boldsymbol{r}; \boldsymbol{R}(t))$ state with quite different energy. In order to avoid this problem, restrictions in the method have been tested. Taking into account the negligible probability that more than two crossing events can take place during the same time interval [t: $t + \Delta t$], the application of the Min-Cost algorithm is limited to values of $\alpha = \beta \pm 2$. Thus, only those $\boldsymbol{\phi}_\alpha(\boldsymbol{r}; \boldsymbol{R}(t+\Delta t))$ states whose energy ordering lies in the window $(\beta - 2, \beta + 2)$ are candidates for assignment to the $\boldsymbol{\phi}_\beta(\boldsymbol{r}; \boldsymbol{R}(t))$ state. In practice, this restriction is implemented by giving arbitrary high values to the corresponding $c_{ij} = -s^2_{\beta\alpha}(t; t+\Delta t)$ matrix elements, thus eliminating the possibility of them being included in the permutation which minimizes the trace given by Eq. (6). Therefore, restrictions in the Min-Cost algorithm is expected to take away some of the efficiency of the method at maximizing the overlaps between the two sets of adiabatic states. In our present work, no significance differences have been observed while applying such restrictions and all our results using either the restricted or unrestricted version of the algorithm have been found equivalent. Let us now discuss its implementation within our recently developed NA-ESMD[60] framework. The state reassignment procedure must be subjected to certain constraints in order to make it compatible with transitions predicted while using the MDQT approach. During the several "trivial" unavoided crossings observed in our NA-ESMD simulations, a wide range of values for the nonadiabatic couplings are obtained depending on the proximity of the current point to the exact crossing point. Therefore, reassignments predicted according to the maximum overlaps can be undone by hops predicted by MDQT according to the strength of the nonadiabatic couplings. In order to resolve this problem, possible reassignments for the current state α are evaluated according to the maximum overlap criteria at each time step during dynamics. If the reassignment algorithm identifies a maximum overlap greater than a certain threshold s_{lim} between the new state α and another old state β, then state α is reassigned to state β, their populations are interchanged, their couplings are cancelled, and the probability to hop is not evaluated. Consequently, the arbitrary effect of the nonadiabatic coupling strength depending on the proximity to the cross point is cancelled. On the other hand, if reassignment of the new state α to the old state β is predicted but the corresponding overlap $s_{\beta\alpha}(t; t+\Delta t)$ is lower than s_{lim}, the quantum time step δt is reduced a certain number of times N_c. Then, we evaluate the existence of any coupling of new and old states that fulfill the requirement that

$$\begin{aligned} s_{\beta\alpha}\left(t + n\frac{\delta t}{N_c}; t + (n+1)\frac{\delta t}{N_c}\right) &\equiv \boldsymbol{\phi}_\beta\left(\boldsymbol{r}; \boldsymbol{R}\left(t + n\frac{\delta t}{N_c}\right)\right) \\ \cdot \boldsymbol{\phi}_\alpha\left(\boldsymbol{r}; \boldsymbol{R}(t + (n+1)\frac{\delta t}{N_c})\right) &> s_{lim}, \end{aligned} \tag{7}$$

with $(n = 0, \ldots, N_c(N_q - 1))$ throughout the time-interval defined by the current classical time step Δt at which a potential unavoided crossing takes place. If not, we interpret that we are in the presence of an unavoided crossing between interacting states and the mixing of states depends on the strength of their nonadiabatic couplings. Therefore, we let the system to evolve on the α state and transition probabilities are evaluated according to the MDQT recipe.

It is important to mention that the value of the threshold s_{lim} actually arbitrarily separates unavoided crossings between interacting states and "trivial" unavoided crossing between noninteracting states. Once the Min-Cost algorithm detects a reassignment, values of $s_{\beta\alpha}(t; t + \Delta t)$ slightly lower than s_{lim} are interpreted as unavoided crossings between interacting states and the corresponding split of electronic populations are subjected to the MDQT algorithm. On the other hand, values of $s_{\beta\alpha}(t; t + \Delta t)$ larger than s_{lim} are considered as "trivial" unavoided crossings between non-interacting states with a probability equal to 1 for the population of the β-state evaluated at t to be reassigned to the α-state evaluated at $t + \Delta t$. Thus, the current adiabatic electronic state is subjected to changes throughout the NA-ESMD simulation either according to hops predicted by the Tully's fewest switches surface-hopping (FSSH) algorithm or according to unavoided crossings detected by the Min-Cost algorithm. It is interesting at this point to mention that the use of the Min-Cost algorithm to track the identity of states is an efficient and robust way to detect unavoided crossings. In principle, no significant gains seem to be achieved respect to the assignment on the simple projection of the current state at the time step i on the basis of the old states at the preceding time step (i-1). Nevertheless, when three or more states are strongly mixed at the same time and, therefore, their identities are changed simultaneously, the simple projection method can lead to erroneous assignments since projections of other states than the current one, are also required. More precisely, a trivial unavoided crossing could take place in situations when two non-interacting α and β states actually interact with other states, impeding the identification of the crossing. In contrast with extremely sharp couplings associated with the "trivial" unavoided crossing between α and β states, couplings with other states can persist for a long time, introducing a substantial state mixture that hinders the identity of states during several time steps along the trajectory. The number of these situations depends on the density of states. Besides, the algorithm is suitable for further treatments of quantum decoherence[68–70] as well as more accurate mixed quantum-classical simulations, involving Ehrenfest trajectories like multiconfigurational Ehrenfest methods[71,72] or the multiple Spawning method,[73] that require the simultaneous identification of "trivial" unavoided crossings involving multiple adiabatic excited states considered during the molecular dynamics simulations.

D. Molecular dynamics simulations

We have studied the photoexcitation and subsequent intra- and/or inter-molecular energy transfer between the fragments of PPE units shown in Figure 1(b). Various distances between fragments have been used in order to test the efficiency of the procedure identifying "trivial" unavoided crossings. Namely, the NA-ESMD simulations have been performed using fragments separated by (a) distance r_f equivalent to that in the original molecule (Figure 1(a)) where the fragments are linked by the three-ring linear PE unit as part of the whole dendritic molecule; and two cases where the same fragments are separated by (b) $r_f = 100$ Å, and (c) $r_f = 500$ Å.

As it was done in the previous studies using the NA-ESMD simulations[52,60,74,75] the Langevin equation at constant temperature[43] with a friction coefficient $\gamma = 2.0$ ps^{-1} was applied[43,74] to simulate the nuclei motions. The initial positions and momenta were taken from a previously equilibrated ground state MD simulations of the entire molecule (Figure 1(a)) during 500 ps trajectory at 300 K using a classical time step $\Delta t = 0.5$ fs. The initial excited state was chosen localized mostly on the fragment of two-ring linear PE segments according to a Frank-Condon window defined as

$$g_\alpha(\mathbf{r}, \mathbf{R}) = \exp\left[-T^2(E_{laser} - \mathbf{\Omega}_\alpha)^2\right], \tag{8}$$

where $E_{laser} = 346$ nm, chosen according to the absorption maximum of the original molecule involving states mainly localized on two-ring linear PE segments. The laser shape is assumed to be a Gaussian $f(t) = \exp(-t^2/2T^2)$, $T^2 = 42.5$ fs, that corresponds to a Gaussian FWHM (Full Width at Half Maximum) of 100 fs. Thus, the initial excited state is selected according to the relative values of the $g_\alpha(\mathbf{r}, \mathbf{R})$ weighted by the oscillator strengths of each state α.

For all simulations, the AM1/CIS level of theory has been used. Previous studies of related systems validate this level of theory by comparison with TDDFT (B3LYP/6-31G*) and experimental results.[26,75] Twenty excited electronic states and their nonadiabatic coupling vectors $\mathbf{d}_{\alpha\beta}$ were included in the simulations. Details on our NA-ESMD implementation and parameters can be found elsewhere.[60] A swarm of 300 NA-ESMD trajectories were propagated during 150 fs at 300 K for each of the previously selected distances between fragments. The nuclei were propagated using the velocity Verlet integration method[76] with a classical time step $\Delta t = 0.1$ fs. Our preliminary calculations have shown that this value of Δt time step is small enough to avoid double crossing events during a unique classical step. A threshold $s_{lim} = 0.9$ was used to define a reassignment detected by the Min-Cost algorithm as an unavoided crossing. Equation (2) is solved using Runge-Kutta-Verner fifth- and sixth-order method as implemented in the NA-ESMD framework.[60] The number N_q of quantum time steps δt per classical time step Δt was 4, and the number of times that δt is reduced, each time a potential trivial unavoided crossing with $s_{\alpha\beta}(t; t + \Delta t) < s_{lim}$ is detected, was $N_c = 10$.

III. RESULTS AND DISCUSSION

During dynamics subsequent to the photoexcitation of polyatomic conjugated molecules, usually multiple unavoided crossings take place. Therefore, electronic states frequently mix and cross between them. This complex dynamics is illustrated in Figure 2, where the evolution in time of the adiabatic energies for 2 manifolds of excited states from the

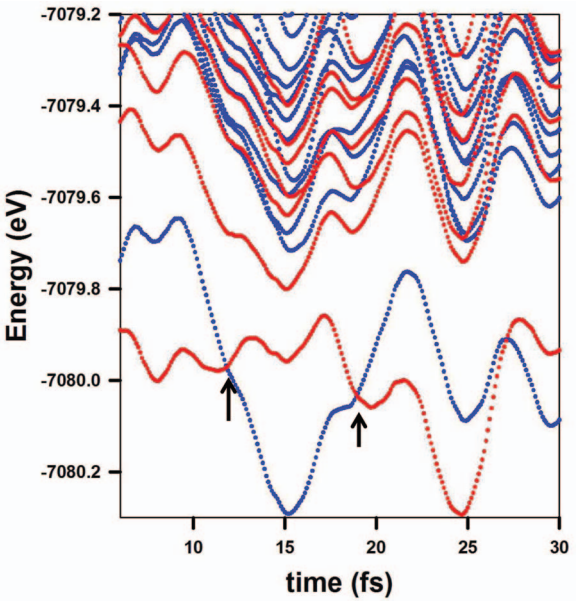

FIG. 2. Variation of the adiabatic energies obtained during a short-time NA-ESMD dynamics of the 2,2-PPE and 4-PPE molecules separated by 100 Å. Blue and red lines correspond to the excited states fully localized on 2,2-PPE and 4-PPE fragments, respectively, as determined by the transition density matrix analysis.

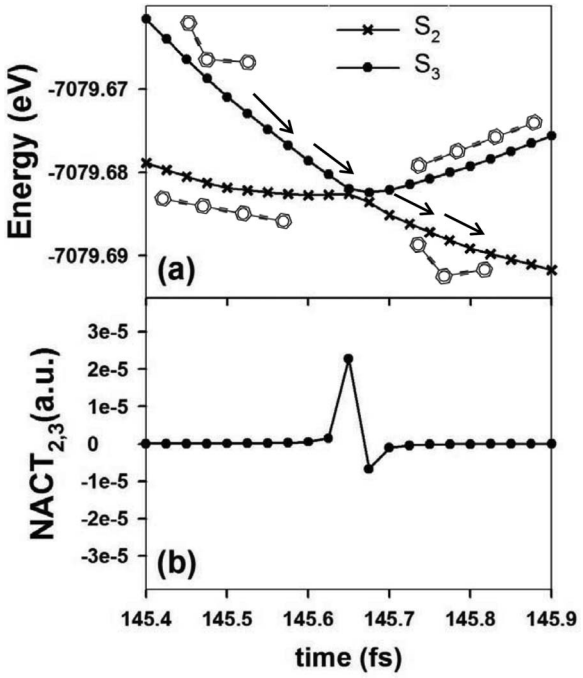

FIG. 3. Typical trivial unavoided crossings between non-interacting adiabatic states obtained from a NA-ESMD simulation of the 2,2-PPE and 4-PPE fragments separated by 500 Å. (a) Time evolution of the adiabatic state energies. The molecular fragments where the transition densities are localized for each state, are also shown. The arrows indicate the dynamics of the system that remains on the same diabatic state. (b) Variation of the respective time-dependent nonadiabatic coupling (NACT) between S_2 and S_3 states.

separated fragments is displayed. Each time when a surface crossing takes place, the adiabatic states given by the energy order may suddenly change their characteristics (for example at any crossing of red and blue lines as indicated with arrows in Figure 2). Here, this has been monitored by following changes in the transition density of the current state occupied according to the MDQT prescriptions. In principle, large values of NACT should be expected at the exact point of crossing where both states become degenerate. Nevertheless, as it has been previously discussed in Sec. II C, this feature is rarely detected during the numerical dynamics propagation. An example of that can be seen in Figure 3(a), where a typical trivial unavoided crossing between non-interacting states, obtained from a NA-ESMD simulation of the 2,2-PPE and 4-PPE molecules separated by 500 Å, is shown. In this example the nuclei initially evolve on the S_3 state before the crossing. This state is fully localized on the 2,2-PPE molecule. As the time evolves, changes in the nuclear geometry make the S_3 state to get close in energy to S_2, whose transition density is fully localized on the 4-PPE molecule. The dynamics continues on S_3 until the nuclei attain a critical geometry corresponding to a region where two states become numerically degenerate. Nevertheless, as both molecules are far apart, it is not expected that these two states interact. Therefore, while the adiabatic states change their energy ordering after the crossing, the nuclei should evolve on the *diabatic pathway* indicated by the arrows in Figure 3(a). Consequently, the *current* state maintains its characteristics throughout the crossing point. Otherwise, an instantaneous and unphysical long-range intermolecular energy transfer could take place in the simulations. According to the MDQT algorithm, a large value of $NACT_{2,3}$ at the "precise" crossing point will guarantee a $S_3 \rightarrow S_2$ transition remaining localized in the 2,2-PPE molecule. Nevertheless, Figure 3(b) shows that the actual values of $NACT_{2,3}$ remain vanishingly small to induce the hop due to a finite time step in numerical simulations.

The issue raised by a simple example above, escalates in large molecules with high density of excited states, where multiple crossings occur not only between interacting or non-interacting states, but also span the intermediate regime. Therefore, if the multiple unavoided crossings are not detected during the NA-ESMD simulations, either unphysical intramolecular energy redistributions or unphysical intermolecular energy transfers can take place. This can be seen by analyzing results obtained from the NA-ESMD simulations without considering any particular treatment of unavoided crossings. Figures (4(a)–4(c)) shows the time evolution of the fractions (averaged over 300 trajectories) of the transition densities localized at each fragment shown in Figure 1(b) when they are separated by different r_f distances. At the shortest separation ($r_f \sim 21$ Å), about 60% population is transferred from the 2,2-PPE to the 4-PPE within 150 fs (Fig. 4(a)). This is expected since at such distances the fragments should be coupled and interactions between the respective transition dipoles should lead to an efficient energy transfer even within a simple Förster theory model. At large separation ($r_f \sim 100$ Å), we also observe a significant ~45% population transfer within 150 fs (Fig. 4(b)), which is counterintuitive given such large separation. Finally, at the largest distance ($r_f \sim 500$ Å), the intermolecular energy transfer results becomes unphysical since the fragments should be uncoupled (Fig. 4(c)), showing the necessity to treat carefully the underlying trivial unavoided crossings.

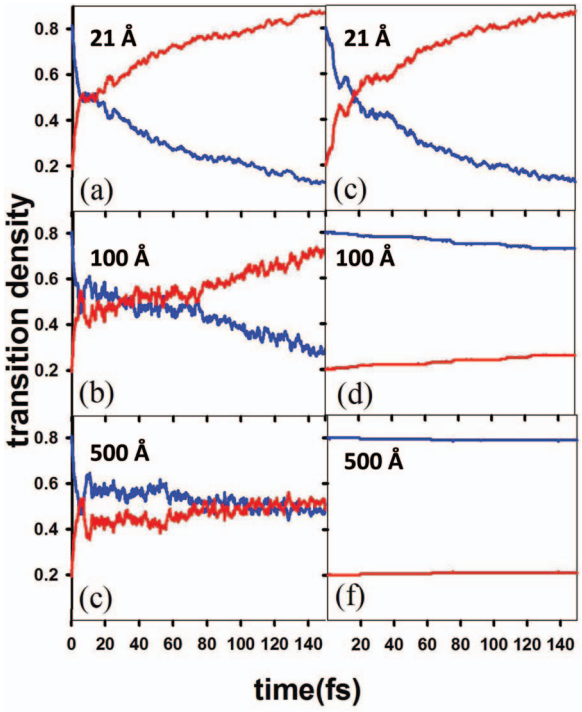

FIG. 4. Variation of the time-dependent fraction of the transition densities localized at the 2,2-PPE (blue lines) and 4-PPE (red lines) fragments when they are separated by different distances. (a), (b), and (c) are obtained from the NA-ESMD simulations without considering any specific treatment of unavoiding crossings. (d), (e), and (f) are obtained from the NA-ESMD simulations including the Min-Cost algorithm dealing with trivial unavoiding crossings.

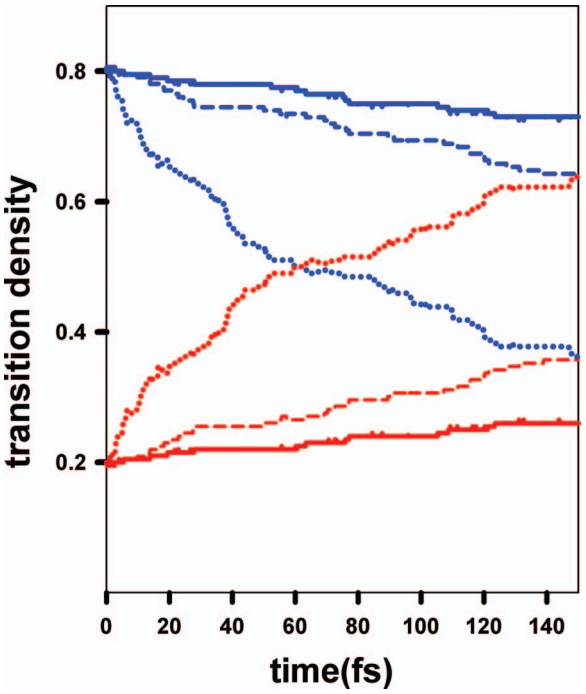

FIG. 5. Comparison of the variation of the time-dependent fraction of the transition densities localized at the 2,2-PPE (blue lines) and 4-PPE (red lines) fragments with $r_f \sim 100$ Å obtained using different procedures: the method proposed in this article (solid lines), a simple projection scheme to detect the trivial unavoided crossings (dashed lines), and an alternative algorithm to deal with cases of $s_{\beta\alpha}(t; t + \Delta t) < S_{\text{lim}}$ (dotted lines).

Indeed, the situation is very different in the case when our new procedure is included in the NA-ESMD simulations. Figure 4(f) shows that, if the two molecules are well separated ($r_f \sim 500$ Å), no changes on the initial average transition density distribution is observed throughout the dynamics, thus reproducing the correct behavior for this limiting case. A similar situation is observed for intermediate intermolecular distances ($r_f \sim 100$ Å) (Fig. 4(e)), where less than 10% of the population is transferred from the 2,2-PPE to the 4-PPE via hops predicted by the MDQT algorithm. At both 500 Å and 100 Å distances, the distribution of radiationless transitions due to crossing (non-interacting states with extremely localized coupling detected by the Min-Cost algorithm) and hopping (interacting states treated by the Tully's fewest switches surface hopping (FSSH) algorithm) is similar, namely ∼88% and ∼12%, respectively. On the other hand, once molecules become coupled ($r_f \sim 21$ Å), both types of NA-ESMD simulations predict similar energy transfer dynamics (compare Fig. (4(a) and 4(d)). Here, the distribution of radiationless transitions due to cross and hop is inverted, being ∼25% and ∼75%, respectively. Nevertheless, the main differences between two simulations appear within ∼10 fs of the dynamics, where the initial intermolecular energy transfer is faster for the dynamics using "hops" only (Fig. 4(a)) without special treatment of trivial unavoided crossing events. Furthermore, similar fast initial intermolecular energy transfers are observed at any distances for this type of dynamics (Figs. 4(a)–4(c)). Thus, presence of trivial crossings affects the excited state dynamics even in the coupled case ($r_f \sim 21$ Å, Fig. 4(a)). The higher density of states at the earliest times during dynamics after photoexcitation, when the system is mainly localized on the highest energy excited states, seems to increase the number of "trivial" unavoided crossing events. Therefore, a failure to treat this effect properly leads to unphysical sudden changes in the spatial localization of the transition density of the current state.

It is interesting at this point to compare our method to two alternative procedures. First, we have tested an algorithm to identify the "trivial" unavoided crossings based on a simple projection of the current state at the time step i to the basis of the old states at the preceding time step (i-1). In Figure 5 we compare the results for the case of two molecules separated by $r_f \sim 100$ Å. The curves corresponding to the 2,2-PPE fragment have been fitted to a simple exponential function of the type $f(t) = A \exp(-t/\tau)$. The resulting values of the energy-transfer time τ were 1500 fs and 685 fs for the curves obtained using the Min-Cost algorithm and the simple projection scheme respectively, pointing out the robustness of the Min-Cost algorithm respect to the simple projection scheme. In addition, we have considered an alternative procedure to deal with situations in which, once a reassignment of the new state α to the old state β is predicted, the corresponding overlap $s_{\beta\alpha}(t; t + \Delta t)$ is lower than s_{lim}. Under these circumstances, the new procedure propagates the quantum coefficient using a reduced quantum time step $\frac{\delta t}{N_c}$, but without evaluating couplings among new and old states that fulfill the requirement given by Eq. (7). That is, we do not allow the possibility to

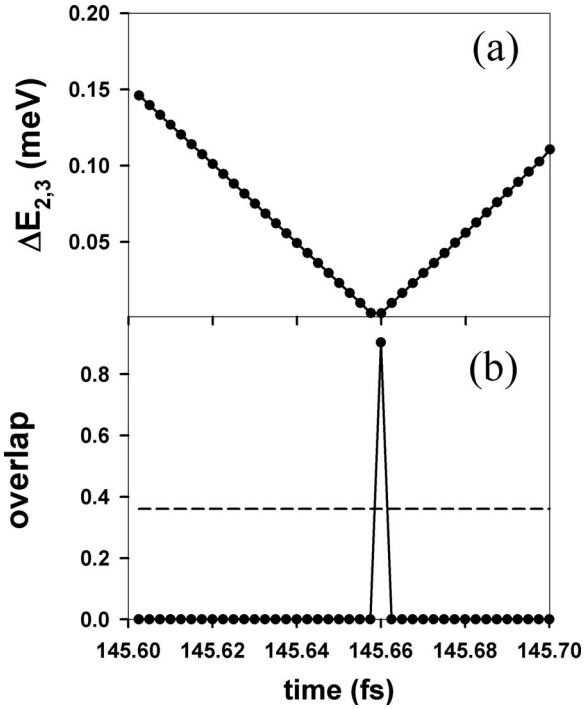

FIG. 6. Time evolution of (a) the energy gap $\Delta E_{\alpha\beta}(t + n\frac{\delta t}{N_c})$, and (b) the overlap $s_{\alpha\beta}(t + n\frac{\delta t}{N_c}; t + (n+1)\frac{\delta t}{N_c})$ with $(n = 0,\ldots, N_c(N_q - 1))$ (see Eq. (7)) throughout the time-interval defined by a classical time step Δt at which a potential unavoided crossing between non-interacting states takes place. The value of the overlap $s_{\alpha\beta}(t; t + \Delta t) \equiv \boldsymbol{\phi}_\alpha(\boldsymbol{r}; \boldsymbol{R}(t)) \cdot \boldsymbol{\phi}_\beta(\boldsymbol{r}; \boldsymbol{R}(t - \Delta t))$ is shown as a dashed line.

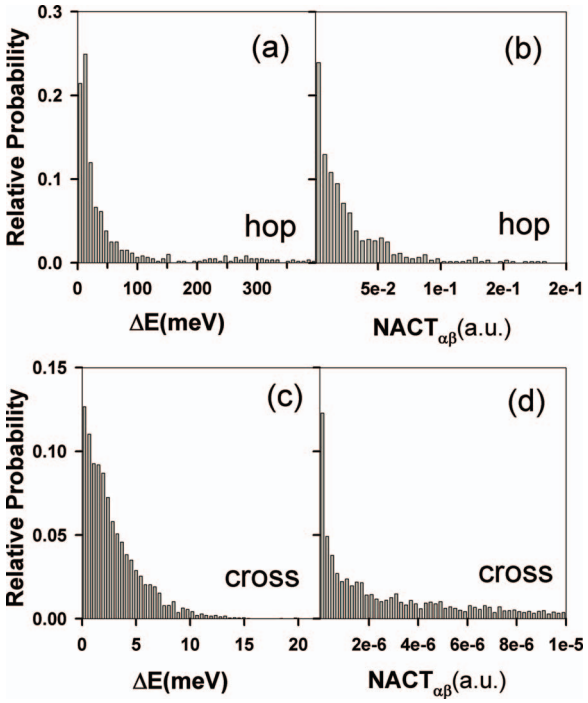

FIG. 7. Distribution of (a) the energy gaps $\Delta E_{\alpha\beta}$ and (b)$NACT_{\alpha\beta}$ at the moment of $S_\beta \rightarrow S_\alpha$ hops, and distribution of (c) energy gaps $\Delta E_{\alpha\beta}$ and (d)$NACT_{\alpha\beta}$at the moment of $S_\beta \rightarrow S_\alpha$ unavoided crossings.

interchange the populations forcing the states to follow the diabatic path. Figure 5 shows that such approach dealing with situations when $s_{\beta\alpha}(t; t + \Delta t) < S_{\text{lim}}$, leads to a significant loss of the number of detected "trivial" unavoided crossings and to a subsequent increase of the unphysical energy transfer between the fragments.

We further discuss cases where the differences between "interacting-state" and "non-interacting-state" crossings become subtle. In the present work, every state reassignment require differentiation between these processes to select an appropriate procedure, i.e., "hops" and "crosses" are treated with the FSSH and Min-Cost algorithms, respectively. In principle, each time a reassignment of a new state α to an old state β is predicted, a value of $s_{\beta\alpha}(t; t + \Delta t) \approx 1$ (or at least $s_{\beta\alpha}(t; t + \Delta t) > S_{\text{lim}}$) should be expected. Nevertheless, we have found several potential reassignments for which $s_{\beta\alpha}(t; t + \Delta t) < S_{\text{lim}}$ At this point, it is important to discern the origin of the low value $s_{\beta\alpha}(t; t + \Delta t)$ from among two possible causes. First, due to finite classical time step, Δt, simulations may simply miss the sharp peaks of the NACTs or, alternatively, the CIS adiabatic functions $\boldsymbol{\phi}_\alpha(\boldsymbol{r}; \boldsymbol{R}(t))$ may change significantly to make $s_{\beta\alpha}(t; t + \Delta t) < S_{\text{lim}}$ On the other hand, the low value of $s_{\beta\alpha}(t; t + \Delta t)$ can be due to a strong mixing of the adiabatic states. While the former can be associated to a trivial unavoided crossing, the latter is related to an interacting-state case. Therefore, in order to distinguish between these scenarios, the quantum time step δt is reduced N_c times and the values of $s_{\beta\alpha}(t + n\frac{\delta t}{N_c}; t + (n+1)\frac{\delta t}{N_c})$are analyzed. Figure 6(b) shows these values within a classical time step Δt at which a typical potential trivial unavoided crossing with $s_{\beta\alpha}(t; t + \Delta t) = 0.36$ takes place. As can be seen, a strongly localized peak is observed when the energy difference between the states reaches its minimum value (Fig. 6(a)), confirming that a trivial unavoided crossing is present here. Such situations have been frequently observed throughout our NA-ESMD simulations. The computational cost of this operation is limited to an additional computation of excited-state energies at each $\frac{\delta t}{N_c}$ time interval. It is important to mention that these situations can be avoided by a direct reduction of the classical time step Δt. Nevertheless, this strategy seems to be impractical since, in the present case, a reduction of Δt by $N_q x N_c$ times is required. On the other hand, the use of variable-step propagators (e.g., Runge-Kutta), assumes additional evaluations of gradients and NACTs.

Let us analyze the main features that characterize the radiationless transitions due to hops and crosses. Figures 7(a) and 7(c) show the distribution of the energy gaps $\Delta E_{\alpha\beta}$ at the moment of $S_\beta \rightarrow S_\alpha$ unavoided crossings between interacting states solved by "hops," and at the moment of $S_\beta \rightarrow S_\alpha$ unavoided crossings between non-interacting states solved by "crosses" obtained from the NA-ESMD simulations of the 2,2-PPE and 4-PPE molecules separated by 500 Å. The average value $\langle \Delta E_{\alpha\beta} \rangle$for hops is 60.7 meV with a maximum of the histogram at 13 meV. On the other hand, two orders of magnitude smaller values are obtained for crosses, where $\langle \Delta E_{\alpha\beta} \rangle$ is 3 meV with a maximum of the histogram at 0.065 meV. These values are significant smaller than the 30 kcal/mol (=1.3 eV) used by Thiel *et al.* as threshold to identify crossing regions when using approximate switching algorithms.[77] It is also smaller than the threshold 0.13 eV to trigger switch of the state tracking in their

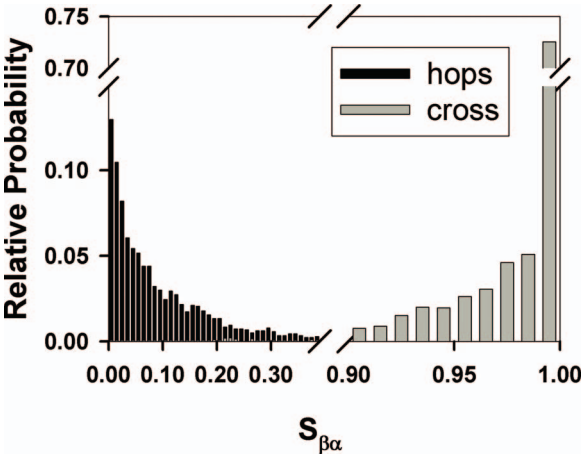

FIG. 8. Histogram of the overlaps $s_{\alpha\beta}(t; t + \Delta t)$ taken at $S_\beta \rightarrow S_\alpha$ hops, and at trivial $S_\beta \rightarrow S_\alpha$ unavoided crossings.

semiempirical implementation of surface hopping molecular dynamics.[64] In our present case, $\sim$ 30% of the crosses take place with $\Delta E_{\alpha\beta} > 1$ kcal/mol (4.3 meV). Furthermore, Figures 7(a) and 7(c) show the differences in the distribution of the values of $NACT_{\alpha\beta}$ between both types of radiationless transitions. Significantly larger values of $NACT_{\alpha\beta}$ are observed during hops compared to crosses. This result confirms that "trivial" unavoided crossing regions cannot be detected *a priori* from the magnitude of $NACT_{\alpha\beta}$ at some time-step. Finally, Figure 8 displays the histograms of the overlaps $s_{\beta\alpha}(t; t + \Delta t)$ at the moment of hops and crosses. On one hand, we can see that, as expected, for trivial unavoided crossings between non-interacting states, the overlaps at crossings remains $\sim$1. That is, the CIS adiabatic functions $\boldsymbol{\phi}_\alpha(\boldsymbol{r}; \boldsymbol{R}(t))$ are not affected by the crossings and preserve their characteristics during crossing event. Furthermore, more than 90% of the overlap values are larger than 0.93, validating the threshold choice ($s_{lim} = 0.9$) in our numerical simulations. In our present example, the choice of values of $s_{lim} > 0.93$ will lead to the missing of more than 10% of the "trivial" unavoided crossings. The situation is opposite on the other end of the spectrum, where most of the "hops" occurs at small values of overlaps (<0.2). Consequently, the histogram in Figure 8 justifies our treatment of every crossing event at either "hop" or "cross" case.

IV. CONCLUSIONS

In this article we present and test a novel numerical procedure based on the Min-Cost algorithm to identify and to treat regions of trivial unavoided crossings between weakly- or non-interacting adiabatic states. The method is particularly suitable for direct "on-the-fly" NA-MD simulations using trajectory surface hopping algorithms that involve a large number of electronic excited states. It exploits the use of analytically computed excited state gradients and non-adiabatic couplings, while identifying "trivial" unavoided crossings events in order to allow the electronic populations to follow the corresponding diabatic pathway. Our algorithm differentiates between crossings between interacting states (simulated by quantum hops), and trivial unavoided crossings between non-interacting states (detected by tracking the states in time with Min-Cost procedure). The outlined method is applicable to dynamics with larger classical time-steps, allowing to deal with "misses" of the sharp peaks of the NACTs as well as significant changes in the time-dependent excited state adiabatic wavefunctions $\boldsymbol{\phi}_\alpha(\boldsymbol{r}; \boldsymbol{R}(t))$ leading to the small overlaps ($s_{\beta\alpha}(t; t + \Delta t) \ll 1$). Consequently, the proposed approach is advantageous to use with Verlet-like algorithms for the propagation of the nuclei during the NA-MD simulations, which allow for larger integration time steps with a reasonable accuracy. Furthermore, our method is inherently designed to be suitable for complex surface hopping implementations and Ehrenfest dynamics that require simultaneous identification of "trivial" unavoided crossings for all electronic states considered during the molecular dynamics simulations.

Molecules of two- and four-ring linear polyphenylene ethynylene (PPE) chromophore units, separated by different distances, are used to test our procedure. The intermolecular energy transfer between both molecules was monitored following changes in the spatial localization of the appropriate electronic transition density matrices of excited states. We have shown that the lack of any special treatment of trivial unavoided crossings during the NA-ESMD simulations leads to unphysical long-range intermolecular energy transfers. However, this is not the case when the new algorithm is included in the NA-ESMD simulations for a variety of intermolecular separations explored. The method also allows the analysis of the distribution of radiationless transitions due to cross ("trivial" unavoided crossings with only extremely sharp couplings at the exact crossing point detected by the Min-Cost algorithm) and hop (unavoided crossings with substantial couplings between the states predicted by the Tully's fewest switches surface hopping (FSSH) algorithm). As expected the former events more dominate at large intermolecular distances. Moreover, the higher density of states at the earliest times during dynamics after photoexcitation, when the system is mainly localized on the highest energy excited states, seems to lead to an increase in the number of "trivial" unavoided crossing events. Finally, the main features that characterize hops and crosses are analyzed. The former have revealed values of $\Delta E_{\alpha\beta}$ and $NACT_{\alpha\beta}$ that are orders of magnitude larger than the latter. Consequently, each of these crossings can be uniquely treated as either "hop" or "cross" case. A numerical comparison of our approach with alternative procedures to either identify or to deal with trivial unavoided crossings has shown the robustness of the procedure.

ACKNOWLEDGMENTS

This work was partially supported by CONICET, UNQ, ANPCyT (PICT-2010-2375) and the National Science Foundation Grant No. CHE-0239120). S.T. and T.N. acknowledge the support of the U.S. Department of Energy through the Los Alamos National Laboratory (LANL) LDRD Program. LANL is operated by Los Alamos National Security, LLC, for the National Nuclear Security Administration of the U.S. Department of Energy (DOE) under contract DE-AC52-06NA25396. We acknowledge support of Center for

qIntegrated Nanotechnology (CINT) and Center for Nonlinear Studies (CNLS) at LANL.

[1]M. Olivucci, *Theoretical and Computational Chemistry 16: Computational Photochemistry* (Elsevier, New York, 2005).
[2]M. Klessinger and J. Michl, *Excited States and Photo-Chemistry of Organic Molecules* (Wiley VCH, Berlin, 1995).
[3]W. Domcke, D. R. Yarkony, and H. Koppel, *Conical Intersections: Electronic Structure, Dynamics & Spectroscopy*, Advanced Series in Physical Chemistry 15 (World Scientific, Sigapore, 2004).
[4]N. J. Turro, V. Ramamurthy, and J. C. Scaiano, *Principles of Molecular Photochemistry: An Introduction* (University Science Books, 2009).
[5]B. Lasorne, G. A. Worth, and M. A. Robb, WIREs Comput Mol Sci. **1**, 460 (2011).
[6]G. A. Worth, M. A. Robb, and B. Lasorne, Mol. Phys. **106**, 2077 (2008).
[7]X. Li, J. C. Tully, and, H. B. Schlegel, J. Chem. Phys. **123**, 084106 (2005).
[8]W. Liang, C. T. Chapman, and X. Li, J. Chem. Phys. **134**, 184102 (2011).
[9]G. A. Worth and M. A. Robb, Adv. Chem. Phys. **124**, 355 (2002).
[10]M. Ben-Nun, J. Quenneville, and T. J. Martinez, J. Phys. Chem. A. **104**, 5161 (2000); M. Ben-Num and T. J. Martinez, Adv. Chem. Phys. **121**, 439 (2002).
[11]I. Burghardt, H. D. Meyer, and L. S. Cederbaum, J. Chem. Phys. **111**, 2927 (1999); G. A. Worth, M. A. Robb, and I. Burghardt, Faraday Discuss. **127**, 307 (2004).
[12]B. Lasorne, M. A. Robb, and G. A. Worth, Phys. Chem. Chem. Phys. **9**, 3210 (2007).
[13]G. Granucci, M. Persico, and A. Toniolo, J. Chem. Phys. **114**, 10608 (2001).
[14]E. R. Bittner, B. J. Schwartz, and P. J. Rossky, J. Mol. Struct. Theochem **389**, 203 (1997).
[15]B. J. Schwartz, E. R. Bittner, O. V. Prezhdo, and P. J. Rossky, J. Chem. Phys. **104**, 5942 (1996).
[16]R. Long and O. V. Prezhdo, J. Am. Chem. Soc. **133**, 19240–19249 (2011).
[17]O. V. Prezhdo, Acc. Chem. Res. **42**, 2005 (2009).
[18]K. Hyeon-Deuk and O. V. Prezhdo, Nano Lett. **11**, 1845 (2011).
[19]B. R. Smith, M. J. Bearpark, and M. A. Robb, Chem. Phys. Lett **242**, 27 (1995).
[20]M. J. Bearpark, F. Bernardi, and M. Olivucci, J. Am. Chem. Soc. **118**, 5254 (1996); M. J. Bearpark, F. Bernardi, and S. Clifford, *ibid.* **118**, 169 (1996).
[21]P. R. L. Markwick and N. L. Doltsinis, J. Chem. Phys. **126**, 175102 (2007).
[22]M. Barbatti, A. J. A. Aquino, J. J. Szymczak, D. Nachtigallová, P. Hobza, and H. Lischka, Proc. Natl. Acad. Sci. U.S.A. **107**, 21453 (2010).
[23]Z. Lan, E. Fabiano, and W. Thiel, J. Phys. Chem.B. **113**, 3548 (2009).
[24]I. Antol, M. Eckert-Maksic, M. Barbatti, and H. Lischka, J. Chem. Phys. **127**, 234302 (2007).
[25]G. Zechmann, M. Barbatti, H. Lischka, J. Pittner, and V. Bonačić-Koutecký, Chem. Phys. Lett. **418**, 377 (2006).
[26]M. Barbatti, G. Granucci, M. Persico, and H. Lischka, Chem. Phys. Lett, **410** 276 (2005); M. Barbatti, M. Ruckenbauer, and H. Lischka, J. Chem. Phys. **122**, 17307 (2005).
[27]M. Pederzoli, J. Pittner, M. Barbatti, and H. Lischka, J. Phys. Chem. A. **115**, 11136 (2011).
[28]T. Cusati, G. Granucci, and M. Persico, J. Am. Chem. Soc. **133**, 5109 (2011).
[29]M. Ruckenbauer, M. Barbatti, B. Sellner, T. Muller, and H. Lischka, J. Phys. Chem. A. **114**, 12585 (2010).
[30]G. Cui and W. Fang, J. Phys. Chem. A. **115**, 1547 (2011).
[31]M. Barbatti, M. Vazdar, A. J. A. Aquino, M. Eckert-Maksić, and H. Lischka, J. Chem. Phys. **125**, 164323 (2006).
[32]M. Barbatti, J. Pittner, M. Pederzoli, U. Werner, R. Mitrić, V. Bonačić-Koutecký, and H. Lischka, Chem. Phys. **375**, 26 (2010).
[33]F. Bernardi, M. Olivucci, and M. A. Robb, Chem. Soc. Rev. **25**, 321 (1996).
[34]G. A. Worth and L. S. Cederbaum, Annu. Rev. Phys. Chem. **44**, 127 (2004).
[35]D. Polli, P. Altoè, O. Weingart, K. M. Spillane, C. Manzoni, D. Brida, G. Tomasello, G. Orlandi, P. Kukura, R. A. Mathies, M. Garavelli, and G. Cerullo, Nature (London) **467**, 440 (2010).
[36]B. G. Levine and T. M. Martinez, Annu. Rev. Phys. Chem. **58**, 613 (2007).
[37]M. Garavelli, P. Celani, F. Bernanrdi, M. A. Robb, and M. Olivucci, M. J. Am, Chem. Soc. **119**, 6891 (1997).
[38]L. M. Frutos, T. Andruniow, F. Santoro, N. Ferre, and M. Olivucci, Proc. Natl. Acad. Sci. U.S.A. **104**, 7764 (2007).
[39]P. Hurd, T. Cusati, and M. Persico, J. Comput. Phys. **29**, 2109 (2010).
[40]C. Evenhuis and T. J. Martinez, J. Chem. Phys. **135**, 224110 (2011).
[41]V. Chernyak and S. Mukamel, J. Chem. Phys. **112**, 3572 (2000).
[42]M. Tommasini, V. Chernyak, and S. Mukamel, Int. J. Quantum Chem. **85**, 225 (2001).
[43]M. Paterlini and D. Ferguson, Chem. Phys. **236**, 243 (1998).
[44]J. Clark, T. Nelson, S. Tretiak, G. Cirmi, and G. Lanzani, Nat. Phys. **8**, 225–231 (2012).
[45]S. Tretiak, A. Saxena, R. L. Martin, and A. R. Bishop, Phys. Rev. Lett. **89**, 097402 (2002).
[46]S. Tretiak, A. Saxena, R. L. Martin, and A. R. Bishop, Proc. Natl. Acad. Sci. U.S.A. **100**, 2185 (2003).
[47]S. Hammes-Schiffer and J. C. Tully, J. Chem. Phys. **101**, 4657 (1994).
[48]J. C. Tully, J. Chem. Phys. **93**, 1061 (1990).
[49]J. C. Tully, "Nonadiabatic molecular dynamics," Int. J. Quantum Chem. **40**, 299 (1991).
[50]S. Tretiak and S. Mukamel, Chem. Rev. **102**, 3171 (2002).
[51]V. Chernyak, M. F. Schulz, S. Mukamel, S. Tretiak, and E. V. Tsiper, J. Chem. Phys. **113**, 36 (2000).
[52]S. Tretiak, C. Isborn, A. Niklasson, and M. Challacombe, J. Chem. Phys. **130**, 054111 (2009).
[53]F. Furche and R. Ahlrichs, J. Chem. Phys. **117**, 7433 (2002).
[54]S. Tretiak and V. Chernyak, J. Chem. Phys. **119**, 8809 (2003).
[55]R. Send and F. Furche, J. Chem. Phys. **132**, 044107 (2010)
[56]S. Mukamel, S. Tretiak, T. Wagersreiter, and V. Chernyak, Science **277**, 781 (1997).
[57]S. Tretiak, V. Chernyak, and S. Mukamel, J. Chem. Phys. **105**, 8914 (1996).
[58]S. Tretiak, W. M. Zhang, V. Chernyak, and S. Mukamel, Proc. Nat. Acad. Sci. U.S.A. **96**,13003 (1999).
[59]M. J. S. Dewar, E. G. Zoebisch, E. F. Healy, and J. J. P. Stewart, J. Am. Chem. Soc. **107**, 3902 (1985).
[60]T. Nelson, S. Fernandez-Alberti, V. Chernyak, A. E. Roitberg, and S. Tretiak, J. Phys. Chem. B, special issue "Mukamel Festschrift" **115**, 5402 (2011).
[61]T. Nelson, S. Fernandez-Alberti, V. Chernyak, A. E. Roitberg, and S. Tretiak, J. Chem. Phys **136**, 054108 (2012).
[62]S. Tretiak, V. Chernyak, and S. Mukamel, J. Am. Chem. Soc. **119**, 11408 (1997).
[63]S. Tretiak, V. Chernyak, and S. Mukamel, Chem. Phys. Lett. **259**, 55 (1996).
[64]E. Fabiano, T. W. Keal, and W. Thiel, Chem. Phys. **349**, 334 (2008).
[65]G. Carpaneto, S. Martello, and P. Toth, Ann. Operat. Res. **13**, 193 (1988).
[66]A. Bastida, M. A. Soler, J. Zuñiga, A. Requena, A. Kalstein, and S. Fernandez-Alberti, J. Chem. Phys. **132**, 224501 (2010).
[67]A. Kalstein, S. Fernandez-Alberti, A. Bastida, M. A. Soler, M. H. Farag, J. Zuñiga, and A. Requena, Theor. Chem. Acc. **128**, 769 (2011).
[68]J. E. Subotnik and N. Shenvi, J. Chem. Phys. **134**, 024105 (2011).
[69]G. Granucci, M. Persico, and A. Zoccante, J. Chem. Phys. **133**, 134111 (2010).
[70]C. Zhu, S. Nangia, A. W. Jasper, and D. G. Truhlar, J. Chem. Phys. **121**, 7658 (2004)
[71]S. K. Reed, M. L. Gonzalez-Martinez, J. Rubayo-Soneira, and D. V. Shalashilin, J. Chem. Phys. **134**, 054110 (2011).
[72]S. K. Reed, D. R. Glowacki, and D. V. Shalashilin, Chem. Phys. **370**, 223 (2010).
[73]M. Ben-Nun and T. J. Martínez, J. Chem. Phys. **108**, 7244 (1998).
[74]S. Fernandez-Alberti, V. D. Kleiman, S. Tretiak, and A. E. Roitberg, J. Phys. Chem. Lett. **1**, 2699 (2010).
[75]S. Fernandez-Alberti, V. D. Kleiman, S. Tretiak, and A. E. Roitberg, J. Phys. Chem A **113**, 7535 (2009).
[76]L. Verlet, Phys. Rev. **159**, 98 (1967).
[77]E. Fabiano, G. Groenhof, and W. Thiel, Chem. Phys. **351**, 111–116 (2008).